THE EFFECT OF TIG WELDING ON CORROSION BEHAVIOR FOR U- BEND SPECIMENS OF 316L AUSTENITIC STAINLESS-STEEL JOINTS IN SALINE SOLUTION

Alaa ABOU HARB [1], Ion CIUCA[2], Mihai VASILE [3], Mohammed Alqasim ALSABTI[4]

Corrosion behavior of three zones in 316L austenitic stainless-steel weld joints (base material BM, heat affected zone HAZ and weld metal WM) was studied in saline solution (5% NaCl) at room temperature. According to the potentiodynamic polarization and the scanning electron microscopy (SEM), some microstructure variation in the BM and HAZ were found.

By comparison between the L316L, LTIGF316L and LTIGV316L specimen, the presence of fatigue fracture in the BM for welded specimens was observed. Topography analysis has evidenced differences in the pits dimensions and shape for each specimen.

Keywords: Austenitic stainless steel, transgranular stress corrosion cracking, saline, pitting corrosion.

1. Introduction

Stress corrosion cracking (SCC) is attributed to metals which work under stress in corrosive environment, and can lead to the metal or alloy cracking under certain conditions [1].

It is known that stainless steel is characterized by the passive layer which forms spontaneously and protects the metal from the aggressive attack of the corrosive media. This layer can be deteriorated due to: (a) presence of heterogeneity in materials during the formation of the alloy e.g. phases, grain boundaries, etc. (b) aggressive elements deposition on the metal's surface e.g. chloride [2].

[1] PhD., faculty of material science and engineering, University POLITEHNICA of Bucharest, Romania, e-mail: alaaabouhareb84@hotmail.com

[2] Prof.univ.dr.ing. Faculty Material Science and Engineering, University POLITEHNICA of Bucharest, Romania, e-mail: ion.ciuca@medu.edu.ro

[3] Conf.dr.ing. Faculty Engineering and Management of Technological Systems, University POLITEHNICA of Bucharest, Romania, e-mail: vasileionmihai@yahoo.com

[4] PhD., faculty of material science and engineering, University POLITEHNICA of Bucharest, Romania, e-mail: mohammedalkasim_faik@yahoo.com

Latest studies have shown that grain boundary and manufacturing conditions (fabrication) which are considered special factors, have enhanced the resistance to stress corrosion cracking, improving so its applications in this field [3].

Studies have indicated that in the stress corrosion cracking, the tensile stress can be diminished when compared to yield stress, indicating that SCC does not appear if the stress is smaller than the critical value, which is called threshold stress. Therefore, residual stresses resulting from welding for example, present lower values than yield stress. On the contrary, residual stresses which exceeds the yield strength value of the alloy, can lead to stress corrosion cracking as of intergranular stress corrosion cracking (IGSCC) and transgranular stress corrosion cracking (TGSCC), or a mixed of the aforementioned [4].

According to the literature, chloride deposits are the most affecting environments for materials and can cause stress corrosion cracking. Among the ions which can affect and cause stress corrosion cracking, the chloride ions are considered the most aggressive, when compared with to bromide, fluoride and iodide ones [5].

One study showed that for 316 and 304 stainless steel, SCC occurs at a temperature of 120°C - 140°C in a solution with 55% lithium bromide [6].

In order to analyze the susceptibility to SCC, the solutions used as electrolytes (e.g. magnesium chloride, sodium chloride and calcium chloride) for tests have been heated to high temperature. Compared with sodium chloride solutions, magnesium and calcium chloride ones appear to be more aggressive for 304/304L stainless steel alloys [7].

It is known that welding technique causes residual stresses in stainless steel and also that the temperature increments is corresponding to a low thermal discharge rate and are considered to be the main causes for its deterioration [8, 9].

Intergranular stress corrosion cracking occurs near heat affected zone, and can be seen as a susceptible area [10].

Our aim was to analyze the stress corrosion cracking and pitting corrosion behavior on austenitic stainless-steel specimens which were welded by tungsten inert gas welding (TIG) technique in saline solutions (NaCl).

2. Experiment

2.1. Materials and methods

For standard stress corrosion cracking the 316L stainless steels specimens were cut with a plasma arc cutting system (model Hypertherm power max 105, Germany) from a sheet of 2000×1000×3 mm. The specimens were obtained from cutting on the longitudinal direction in respect to the rolling direction of the steel sheet. The tested specimen's dimensions are 100×9×3 mm (three specimens). The

chemical compositions of the alloys used in the present study are shown in Table 1.

Table 1

Chemical composition of the alloy (wt. %)

Materials	C	Si	Mn	P	S	Cr	Ni	Mo	Cu
316L	**0.018**	**0.406**	**1.88**	**0.019**	**0.0029**	**17.04**	**9.55**	**1.85**	**0.391**

The samples dimensions used for stress corrosion cracking tests are illustrated in Fig. 1.

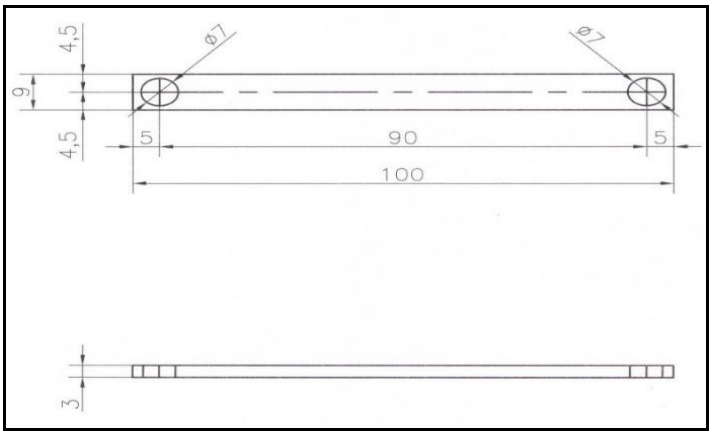

Fig.1. Dimension of the samples used in stress corrosion cracking experiments

Two specimens were cut in the middle by using a traditional shearing equipment, after which the two halves were welded together by TIG. Welding parameters are shown in Table 2.

Table 2

Welding parameters used

specimens	Welding method	Welding current (A)	Shielding gas	Welding voltage (V)	Welding wire
Full specimens					
LTIG 316L	TIG	80	Argon	20 - 24	316L

The samples for stress corrosion cracking tests have been designed according to ASM, with a U-band aspect (Fig. 2) [4].

In Fig. 3 are presented the macroscopic images of the obtained samples as follows: the first specimen is L316L (without welding), the second specimen is LTIGF316L (face bend) and the third specimen is LTIGV316L (root bend). Sample coding reflects the used welding process, TIG - tungsten inert gas

welding, the alloy-316L; sample orientation, L – longitudinal. Bending method for the welded surface, F – face bend, V- root bend.

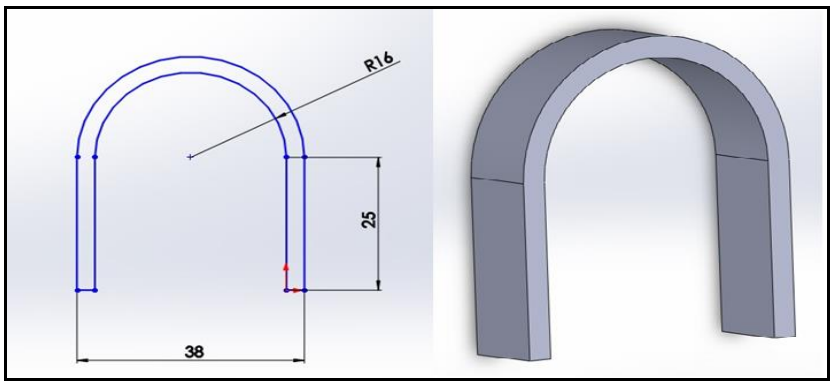

Fig.2. Dimension of standard U-bend specimens used in SCC testing

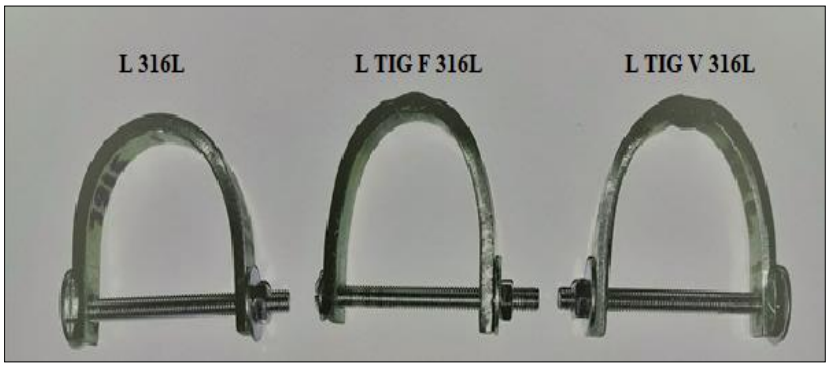

Fig.3. Standard U-bend specimens used in SCC testing of AISI 316L austenitic stainless steels

2.2. Corrosion test

Corrosion behavior was determined by linear polarization technique that involves the following steps:

- measuring the open circuit potential (OCP), over a period of 3 hours;
- registering the potentiodynamic polarization curves from -1V (vs E_{OC}) to +1V (vs E_{ref}) at a scanning rate of 1 mV/s.

The corrosion behavior tests were performed by using a Potentiostat/Galvanostat (model PARSTAT 4000, Princeton Applied Research, USA), equipped with the VersaStudio software. Tests were performed in saline solution 5% NaCl, at room temperature.

2.3. SEM/EDX

Surface analysis has been done by using a scanning electron microscope (SEM) and the chemical composition has been done by using an energy dispersive X-Ray spectrometer (EDX).

2.4. Depth of corrosion

ImageJ (IJ 1.51K) program has been used to determine the pit dimensions, such as depth and radius [11].

3. Results

3.1. Corrosion behavior

In Fig. 4 are presented the open circuit potential variation (E_{oc}) and the potentiodynamic polarization curves.

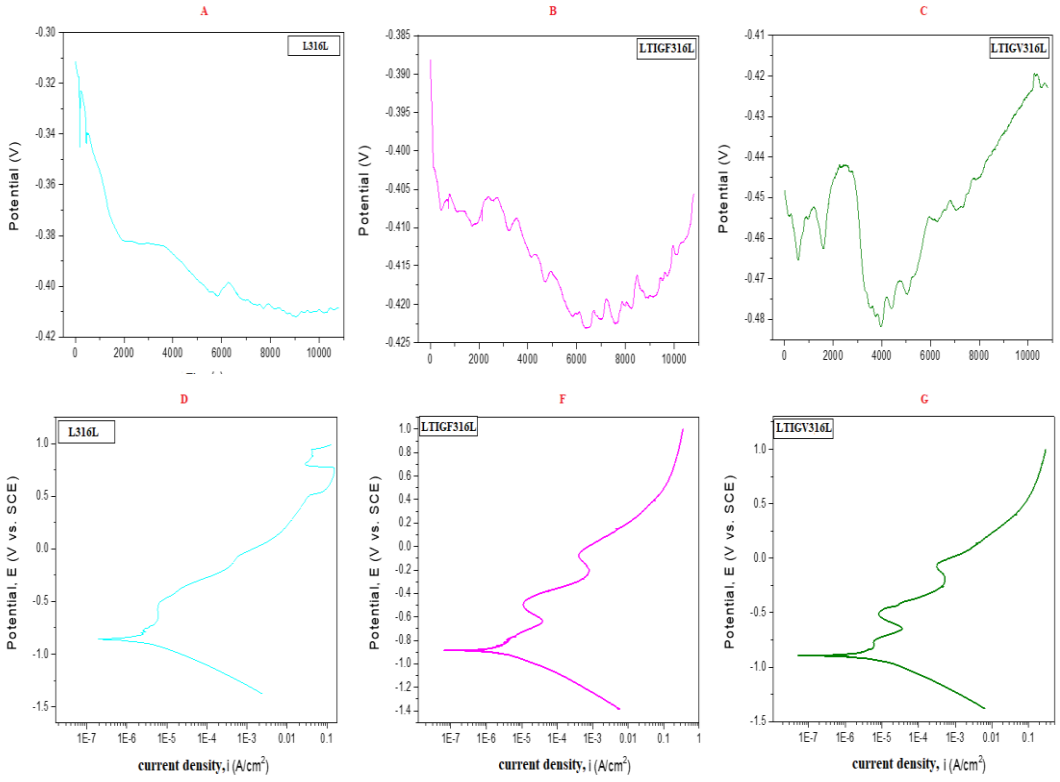

Fig.4. Evolution of the open circuit potential (OCP) for (A) L316L (B) LTIGF316L (C) LTIGV316L and potentiodynamic curves for (D) L316L (F) LTIGF316L (G) LTIGV316L

From the open circuit potential evolution and Tafel extrapolation from the potentiodynamic curves, the following parameters characterizing the corrosion resistance of the investigated specimens were obtained:

- open circuit potential (E_{oc});
- corrosion potential (E_{corr});
- corrosion current density (i_{corr}).

Table 3 shows the main parameters of the electrochemical corrosion process.

Table 3

The main parameters of the corrosion process

Specimens	Samples codification	E_{oc} (mV)	E_{corr} (mV)	i_{corr} (μA/cm^2)
U-316L	L 316L	-396	-856	3,300
U-316L	L TIG F 316L	-395	-886	2,797
U-316L	L TIG V 316L	-392	-893	7,437

The corrosion resistance of the experimental samples was examined based on several evaluation criteria.

If we consider the value of the open circuit potential (E_{oc}), it is known that a more electro-positive value shows a better corrosion behavior. Electrochemical measurements showed that for the 316L alloy, the most electro-positive value is obtained for the LTIGV316L sample, even though the values of all three specimens are similar, with differences of a few mV.

From the point of view of the corrosion potential (E_{corr}), it is considered that the more electro-positive values show a better corrosion behavior. According to this criterion, the L316L has the most electro-positive value followed by LTIGF316L and LTIGV316L. For the last two, it was noted that the corrosion potential presents close values.

A low corrosion current density indicates a good corrosion resistance. Thus, considering this criterion, the lowest value of the corrosion current density is obtained for the LTIGF316L specimen with a value of 2,797 μA/cm^2, followed L316L and LTIGV316L which have registered values of 3,300 μA/cm^2 and 7,437 μA/cm^2, respectively.

3.2. SEM/EDX

Fig 5, 6 and 7 show SEM/EDX micrographs of L316L, LTIGF316L and LTIGV316L alloys used in this study. From the SEM images presented in Fig 5, some defects that are indicated by yellow arrows can be observed (pitting corrosion).

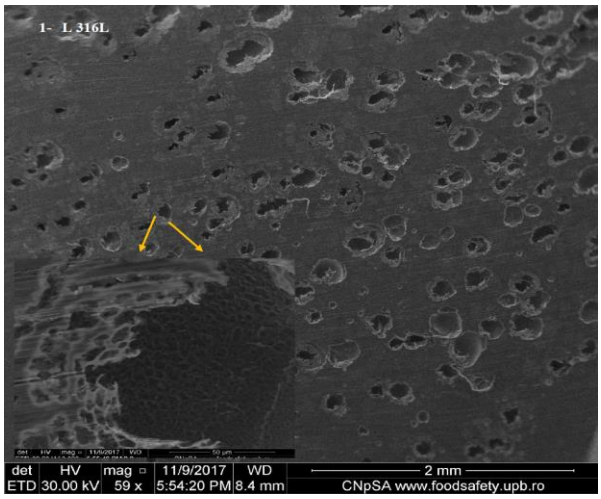

Fig.5. SEM image of the U-L316L specimen

As it can be seen in Fig. 6, we studied three zones: base material, heat affected zone (HAZ) and weld metal as follows:

- **A zone** (base material): from the SEM result of the U-LTIGF316L specimen, fatigue beach marks are observed indicating a possible fatigue fracture;
- **B zone** (HAZ): some fatigue lines have been noted in the fatigue fracture surface;
- **C zone** (weld metal): by SEM result, we found that there is rectangular defect similar to pitting in the marginal areas;
- **D zone** (HAZ): due to several factors such as thermal stresses by welding process and stresses by bend test, grain boundary fracture caused by transgranular fracture and brittle particles can be observed;
- **E zone** (base material): some pitting corrosion and fatigue fracture (fatigue beach marks) were observed in this region, and are in accordance with other literature data [12].

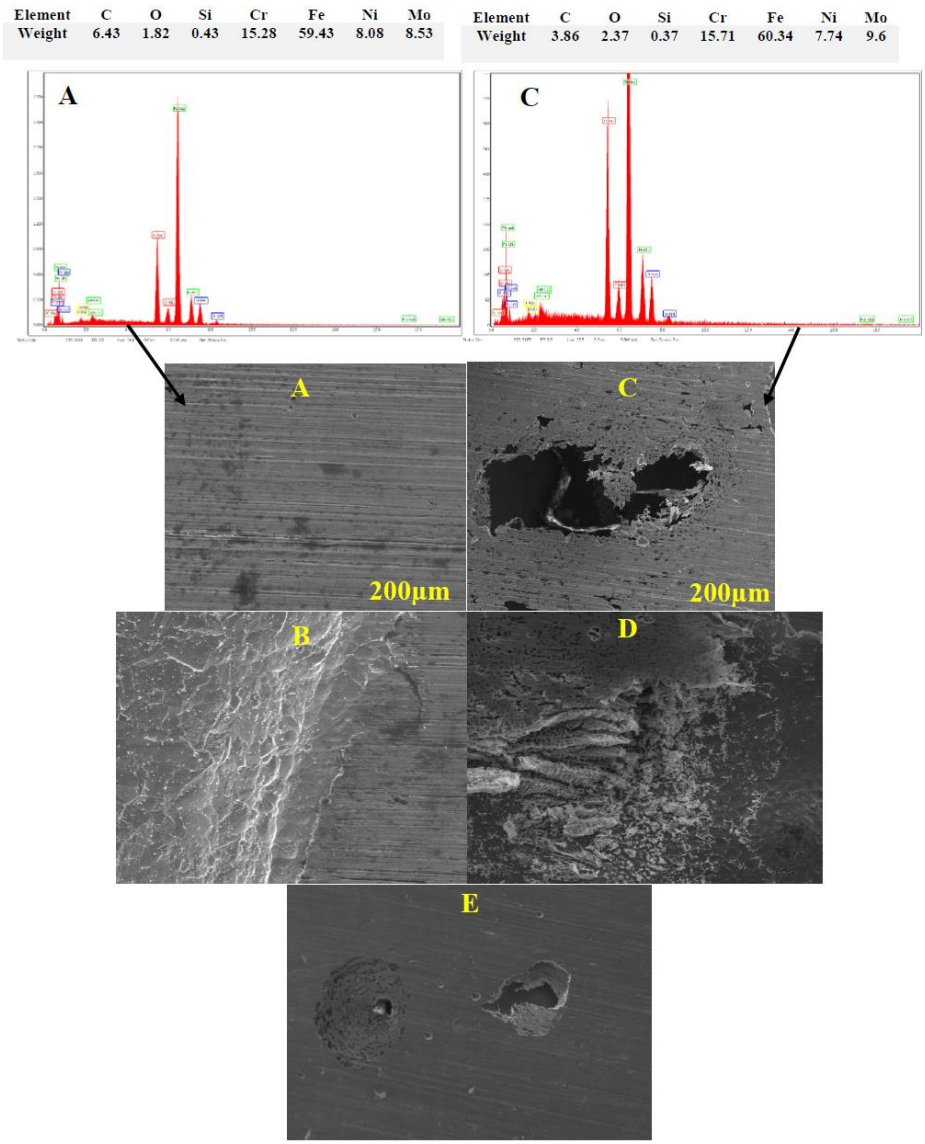

Fig.6. SEM images and EDX spectra of the face bend for U-LTIGF316L alloy: A) base material B) HAZ C) weld metal D) HAZ and E) base material

In **A** and **C zone** of the LTIGF316L alloy (base material zone and weld metal zone) the peaks for C, O, Si, Cr, Fe, Ni, and Mo elements are present. An increased carbon content and decreased oxygen content in the A zone, by comparison with the C zone, has also been observed.

In Fig. 7, three regions have been investigated and the following were observed:

- **A zone** (base material): from SEM images of the U-LTIGF316L specimen, fatigue beach marks are observed indicating a possible fatigue fracture;

- **B zone** (weld metal): some fatigue lines have been noted in the fatigue fracture surface;
- **C zone** (HAZ): some fatigue lines in the fatigue fracture surface were identified.

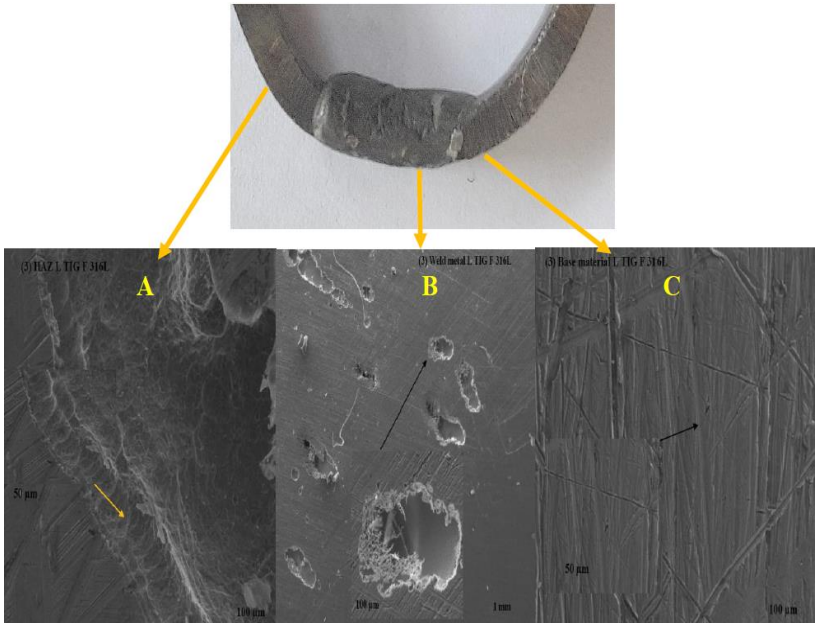

Fig.7. SEM images of the face bend for U-LTIGV316L alloy: A) base material B) weld metal C) HAZ

3.3. Dimensions of pits

Fig. 8 shows 3D image for one of the pits, and the curve of its topography for all specimens.

We notice that the depth of the pit for L316L is approximately 50 µm, while for LTIGF316L and LTIGV316L values of 80 µm and 40 µm, respectively have been regestered. According to this it can be said that 316L alloy presents a better corrosion resistance to pitting corrosion in seawater, especially in stagnant water. By comparison the specimens U-L316L, U-LTIGF316L and U-LTIGV316L in terms of pits topography, some similarities regarding the pits shape presented in ASTM were remarked.

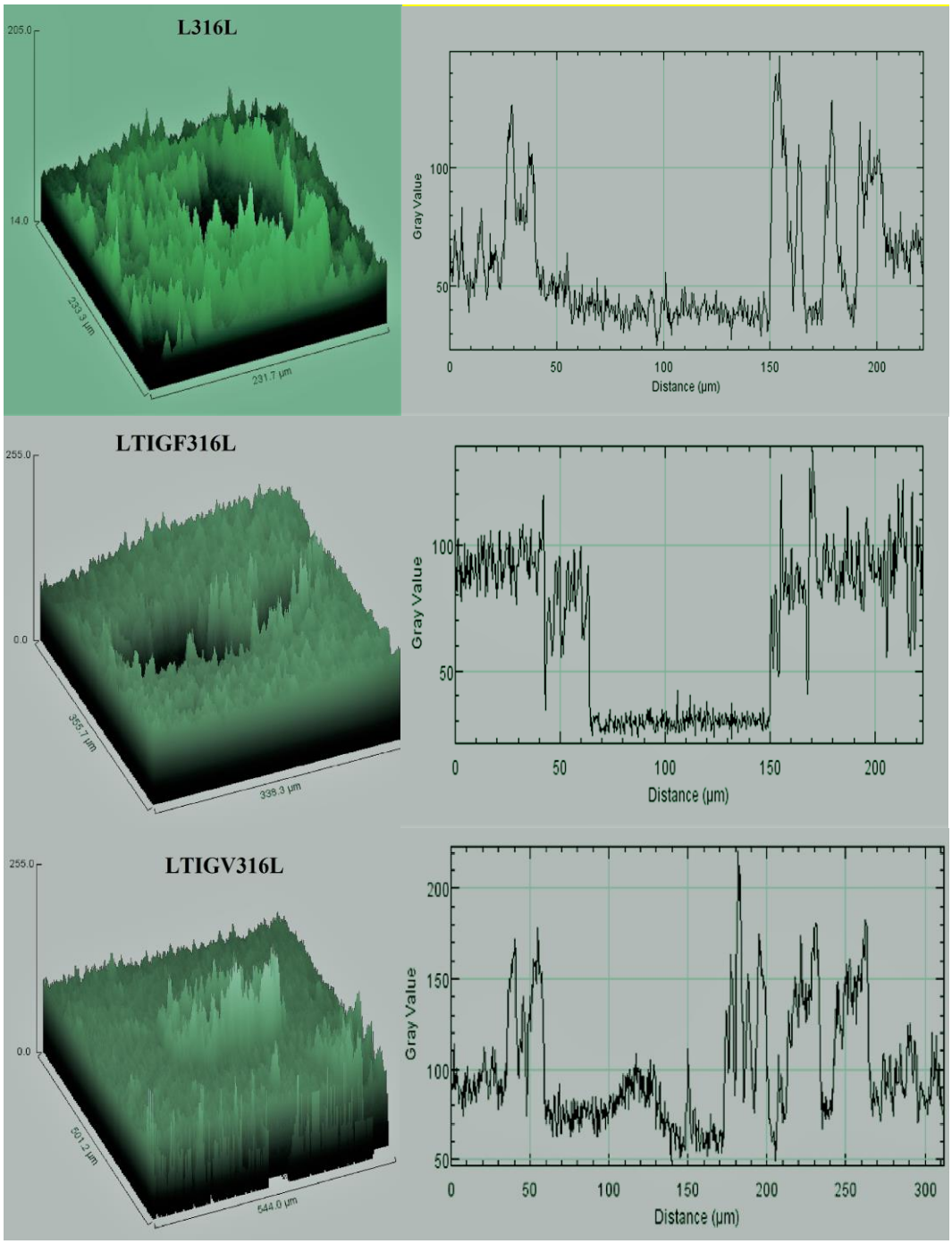

Fig.8. Pitting topography for L316L, LTIGF316L and LTIGV316L specimens

4. Discussion and conclusion

From the electrochemical result, the lowest value of the corrosion current density is obtained for the LTIGF316L specimen with a value of (2.797 μA/cm^2) followed by L316L (3.300 μA /cm^2) and LTIGV316L specimen (7.437 μA /cm^2).

Scanning Electron Microscopy (SEM) was used to observe the samples morphology which revealed the presence of pitting corrosion for L316L (without welding).

Fracture at grain boundary has been noticed in the heat affected zone for LTIGF316L samples which emerged as a result of transgranular fracture and brittle particles due to several factors such as thermal stresses from the welding process, and the stresses induced by the bend test.

On the LTIGV316L sample, both fatigue fracture as well as rectangular pitting defect have been found in the welded metal zone. Differences regarding their dimension and shape were observed when studying the pits topography for each sample.

The electrochemical results have evidenced that the sample LTIGF316L has a better corrosion resistance especialy for the base material and the heat affected zone, indicating that this can be a material of choice in the industrial applications.

R E F E R E N C E S

[1] X. Guo, K. Chen, W. Gao, Z. Shen, P. Lai, and L. Zhang, “A research on the corrosion and stress corrosion cracking susceptibility of 316L stainless steel exposed to supercritical water,” *Corros. Sci.*, vol. 127, no. August, pp. 157–167, 2017.

[2] V. Kain, *Stress corrosion cracking (SCC) in stainless steels*. Woodhead Publishing Limited, 2011.

[3] J. A. Beavers, F. Gui, and N. Sridhar, “Effects of environmental and metallurgical factors on the stress corrosion cracking of carbon steel in fuel-grade ethanol,” *Corrosion*, vol. 67, no. 2, pp. 0250051–02500515, 2011.

[4] G. S. Frankel, “Corrosion: Fundamentals, Testing, and Protection,” *ASM Handb.*, vol. 13A, pp. 44073–2, 2003.

[5] J. Klinglmayr and C. Bettstetter, “Low temperature stress corrosion cracking of austenitic and duplex stainless steels under chloride deposits,” 2001.

[6] D. Itzhak and O. Elias, “Behavior of type 304 and type 316 austenitic stainless steels in 55% lithium bromide heavy brine environments,” *Corrosion*, vol. 50, no. 2, pp. 131–137, 1994.

[7] M. O. Speidel, “Stress corrosion cracking of stainless steels in NaCl solutions,” *Metall. Trans. A*, vol. 12, no. 5, pp. 779–789, 1981.

[8] J. Xu, J. Chen, Y. Duan, C. Yu, J. Chen, and H. Lu, “Comparison of residual stress induced by TIG and LBW in girth weld of AISI 304 stainless steel pipes,” *J. Mater. Process. Technol.*, vol. 248, no. May, pp. 178–184, 2017.

[9] T. Simson, A. Emmel, A. Dwars, and J. Böhm, “Residual stress measurements on AISI 316L samples manufactured by selective laser melting,” *Addit. Manuf.*, vol. 17, pp. 183–

189, 2017.
[10] C. Ma, Q. Peng, J. Mei, E.-H. Han, and W. Ke, "Microstructure and Corrosion Behavior of the Heat Affected Zone of a Stainless Steel 308L-316L Weld Joint," *J. Mater. Sci. Technol.*, no. 2010, 2017.
[11] R. B. Ribeiro *et al.*, "Morphology Characterization of Pitting Corrosion on Sensitized Austenitic Stainless Steel by Digital Image Analysis," vol. 6.
[12] A. P. Serra, "World â€™ s largest Science , Technology & Medicine Open Access book publisher," *Biomass Now- Sustain. growth use*, 2013.